Bench Test of Range Extension Autonomous Driving for Electric Vehicles Based on Optimization of Velocity Profile Considering Traffic Signal Information

Hiroshi Fujimoto[1)] **Hideki Yoshida**[1)] **Daisuke Kawano**[2)] **Yuichi Goto**[2)]
Misaki Tsuchimoto[3)] **Koji Sato**[3)]

1) The University of Tokyo, 5-1-5 Kashiwanoha, Kashiwa, Chiba, 277-8561 Japan
2) National Traffic Safety and Environment Laboratory 7-42-27, Jindaijihigashimachi Chofu, Tokyo, 182-0012, Japan
3) Ono Sokki Co., Ltd. 1-16-1, Hakusan, Midori-ku, Yokohama Kanagawa, 226-8507, Japan

Presented at the EVTeC and APE Japan on May 22, 2016

ABSTRACT: Electric Vehicles (EVs) are recognized as a practical solution for environmental and energy problems. The mileage per charge of EVs, however, is shorter than the mileage of Internal Combustion Engine Vehicles (ICEVs). In this paper, Range Extension Autonomous Driving (READ) system considering the traffic signal information is proposed. The proposed system optimizes the velocity profile of autonomous driving based on the precise loss models of vehicles. The authors carried out simulations and experiments that proved the effectiveness of the proposal in terms of mileage per charge.

KEY WORDS: electric vehicle, range extension autonomous driving, traffic signal information, nonlinear optimization

1. Introduction

Electric Vehicles (EVs) have been attracting an increasing attention as one of the solutions for global environmental and energy problems. In adittion, EVs are superior to Internal Combustion Engine Vehicles (ICEVs) in terms of motion control [(?)]. The mileage per charge of EVs, however, is shorter than the mileage of ICEVs. To solve this problem, various methods were proposed [(?) (?) (?) (?) (?)]. For examples, in (**?**), motor efficiency is improved by utilizing individual winding current control. In (**?**), the authors proposed an optimization algorithm to distribute front and rear driving/braking forces by considering the slip ratio and the motor loss. It should be noted that, these studies focused on vehicles driven by drivers.

Thanks to the advances in Intelligent Transport Systems(ITS), Infrastructure-to-Vehicle (I2V) communications can provide fast and cheap Advanced Driving Assistance System (ADAS) [(?)]. In the near future, vehicle velocity is determined by autonomous driving system from ITS information and traffic environment. Various research groups have proposed the optimization of vehicle velocity profile to reduce total energy consumption [(?) (?)]. However most of these research did not deal with the short mileage per charge of EVs. In (**?**), energy consumption was reduced by optimizing velocity profile and considering the traffic signal information on the assumption that ITS provides the traffic signal information in advance. Yet these research did not consider iron loss and slip loss.

The authors' research group has proposed Range Extension Autonomous Driving (READ) using purely motion control techniques [(?) (?) (?)], which does not change motor type and vehicle structures. READ can reduce energy consumption by optimizing velocity profile. However, conventional READ did not consider important factors such as the traffic signal information. READ considering the traffic signal information can be expected to reduce more energy consumption. In this study, the traffic signal information is assumed to be available from optical beacon, and the velocity profile can be designed by solving a nonlinear optimal control algorithm. The effectiveness of proposed method is verified by simulations and experiments.

Fig. 1: FPEV2–Kanon.

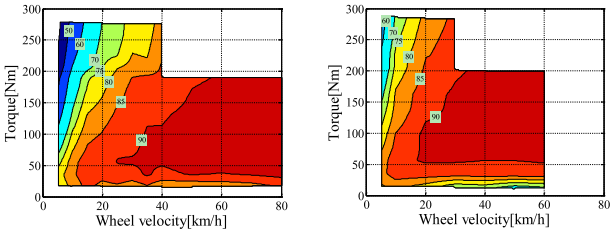

(a) Front motor. (b) Rear motor.

Fig. 2: Efficiency maps of front and rear motors.

2. Experimental Vehicle and Model

2.1. Experimental Vehicle

In this research, an original electric vehicle "FPEV2–Kanon" manufactured by the authors' research group is used. The picture and the specification of the vehicle are shown in Fig. 1 and Tab. **??**, respectively. This vehicle has four outer–rotor type in–

Copyright © 2016 Society of Automotive Engineers of Japan, Inc. All rights reserved

Table 1: Vehicle specification.

Meaning	Symbol	Value
Vehicle mass	M	854 kg
Wheel base	l	1.72 m
Distance from CG to front axle	l_f	l_f : 1.01 m
Distance from CG to rear axle	l_r	l_r : 0.702 m
Front wheel inertia	$J_{\omega f}$	1.24 kgm^2
Rear wheel inertia	$J_{\omega r}$	1.26 kgm^2
Wheel radius	r	0.302 m

Table 2: Specifications of in–wheel motors.

	Front	Rear
Manufacturer	TOYO DENKI SEIZO K.K.	
Type	Direct drive system Outer rotor type	
Rated torque	110 Nm	127 Nm
Maximum torque	500 Nm	530 Nm
Rated power	6.00 kW	6.00 kW
Maximum power	20.0 kW	25.0 kW
Rated speed	382 rpm	450 rpm
Maximum speed	1110 rpm	1200 rpm

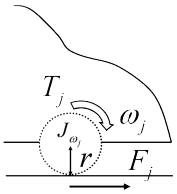

(a) Rotational motion of a wheel.

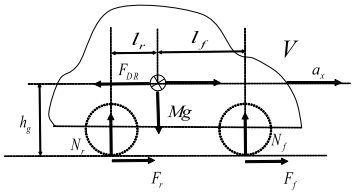

(b) Load transfer model.

Fig. 3: Vehicle model.

wheel motors. These motors are direct drive type. Therefore the reaction forces from the road are directly transferred to the motor without the backlash influence of the reduction gear. Tab. **??** and Fig. **??** show the specification of the motors and efficiency maps of the front and the rear in–wheel motors, respectively. Lithium-ion battery is used as power source. The voltage of the main battery is 160 V. The voltage is boosted to 320 V by a converter. In this paper, the converter loss is assumed to be negligible small.

2.2. Vehicle Model

In this section, a four wheel driven vehicle model is described. Using the model given in Fig. **????**, the wheel dynamics is expressed as Eq.(**??**). From Fig. **????**, the vehicle dynamics are expressed as Eq.(**??**)–(**??**)

$$J_{\omega_j}\dot{\omega}_j = T_j - rF_j, \tag{1}$$

$$M\dot{V} = F_{\rm all} - {\rm sgn}(V)F_{\rm DR}(V), \tag{2}$$

$$F_j = \frac{1}{4}F_{all}, \tag{3}$$

$$F_{\rm DR}(V) = \mu_0 Mg + b|V| + \frac{1}{2}\rho C_{\rm d} A V^2, \tag{4}$$

where ω_j is the wheel angular velocity, V is the vehicle velocity, T_j is the motor torque, F_j is the driving force of each wheel, $F_{\rm all}$ is the total driving force, M is the vehicle mass, r is the wheel radius, J_{ω_j} is the wheel inertia, $F_{\rm DR}$ is the driving resistance, μ_0 is rolling friction coefficient, b is resistance vehicle velocity coefficient, ρ is air density, $C_{\rm d}$ is drag coefficient and A is frontal projected area. The subscript j represents f or r, f stands for "front" and r represents "rear".

The slip ratio λ_j is defined as

$$\lambda_j = \frac{V_{\omega_j} - V}{\max(V_{\omega_j}, V, \epsilon)}, \tag{5}$$

where $V_{\omega_j} = r\omega_j$ is the wheel speed and ϵ is a small constant to avoid zero division. The slip ratio λ_j is known to be related with the friction coefficient μ_j [?]. In the region $|\lambda_j| \ll 1$, μ_j is nearly proportional to λ_j. Then, for longitudinal acceleration cases,

$$F_j = \mu_j N_j \approx D_s^{'} N_j \lambda_j, \tag{6}$$

where N_f and N_r are respectively the front and rear normal forces, $D_s^{'}$ is the normalized driving stiffness.

The normal forces of each wheel during the longitudinal acceleration process are calculated as follows

$$N_f(\dot{V}) = \frac{1}{2}\left[\frac{l_r}{l}Mg - \frac{h_g}{l}M\dot{V}\right], \tag{7}$$

$$N_r(\dot{V}) = \frac{1}{2}\left[\frac{l_f}{l}Mg + \frac{h_g}{l}M\dot{V}\right], \tag{8}$$

where l_f and l_r are respectively the distances from the center of gravity to the front and rear axles, l is the wheelbase, and h_g is the height of the center of gravity.

2.3. Power Flow Model [?]

The inverter input power $P_{\rm in}$ considering the slip ratio and motor loss is expressed as

$$P_{\rm in} = P_{\rm out} + P_{\rm c} + P_{\rm i}, \tag{9}$$

where $P_{\rm out}$ is the sum of the mechanical outputs of each motor, $P_{\rm c}$ is the sum of the copper losses of each motor, and $P_{\rm i}$ is the sum of the iron losses of each motor. The inverter loss is assumed to be negligible small.

When each wheel angular acceleration is small, torque T_j is proportional to driving force. T_j can be expressed as

$$T_j \approx rF_j. \tag{10}$$

When the slip ratioλ_j is small enough, ω_j is expressed as

$$\omega_j = \frac{V}{r(1-\lambda_j)} \approx \frac{V}{r}(1+\lambda_j). \tag{11}$$

Then, λ_j is expressed as

$$\lambda_j = \frac{F_j}{D_s' N_j(\dot{V})} = \frac{F_{\rm all}}{4D_s' N_j(\dot{V})}. \tag{12}$$

Therefore $P_{\rm out}$, $P_{\rm c}$ and $P_{\rm i}$ can be expressed as

$$P_{\rm out} = 2\sum_{j=fr} \omega_j T_j,$$

Copyright © 2016 Society of Automotive Engineers of Japan, Inc. All rights reserved

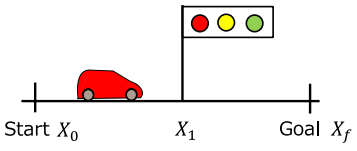

(a) Assumed scenario.

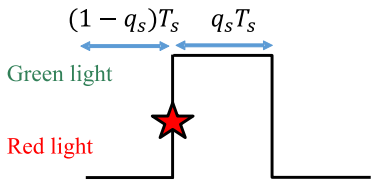

(b) Traffic signal information.

Fig. 4: Assumed scenario and Traffic signal information.

$$\simeq V\frac{F_{\rm all}}{2}\sum_{j=f,r}\left(1+\frac{F_{\rm all}}{4D_s'N_j(\dot{V})}\right), \tag{13}$$

$$P_{\rm c}=2\sum_{j=f,r}R_j{i_{qj}}^2=\frac{r^2}{8}{F_{\rm all}}^2\sum_{j=f,r}\frac{R_j}{{K_{tj}}^2}, \tag{14}$$

$$P_{\rm i}=\frac{2V^2}{r^2}\sum_{j=f,r}\frac{{P_{nj}}^2}{R_{cj}}\left[\left(\frac{rL_{qj}F_{\rm all}}{4K_{tj}}\right)^2+{\Psi_j}^2\right], \tag{15}$$

where R_j is the armature winding resistance of the motor, K_{tj} is the torque coefficient of the motor, P_{nj} is the number of pole pairs, L_{qj} is the q–axis inductance and Ψ_j is the interlinkage magnetic flux.

The electrical angular speed of the motor ω_{ej} and the equivalent iron loss resistance R_{cj} are expressed as

$$\omega_{ej}=\frac{P_{nj}V}{r}, \tag{16}$$

$$\frac{1}{R_{cj}}=\frac{1}{R_{c0j}}+\frac{1}{{R_{c1j}}'|\omega_{ej}|}, \tag{17}$$

where the first and second terms on the right–hand side represent the eddy current loss and hysteresis loss, respectively.

Therefore, the inverter input power is expressed by V and $F_{\rm all}$ as

$$P_{\rm in}(V,F_{\rm all})=P_{\rm out}(V,F_{\rm all})+P_{\rm c}(F_{\rm all})+P_{\rm i}(V,F_{\rm all}). \tag{18}$$

3. Optimization of Velocity profile Considering Traffic Signal Information

In this section, we assumed that the autonomous driving systems are installed with EVs and proposed the READ. It calculates optimal velocity profile which minimizes the total amount of energy consumption from initial time t_0 to final time t_f. In this paper, we assume that the vehicle runs at $V_0 = 30.0$ km/h by the starting point $X_0 = 0.00$ m and will stop with $V_f = 0.00$ km/h at the goal $X_f = 400$ m.

3.1. Signal Information Model

In this example, the traffic light is assumed to be installed at $X_1 = 200$ m. The traffic signal information model of the traffic signal is represented as

$$\mathrm{s}(t,X_1)=\begin{cases}0 & (0\leqq t\leqq(1-q_{\rm s})T_{\rm s})\\ 1 & ((1-q_{\rm s})T_{\rm s}<t\leqq T_{\rm s}),\end{cases} \tag{19}$$

where $\mathrm{s}(t,X_1)$ is the traffic signal information at $X_1 = 200$ m, $T_{\rm s}$ is one cycle, $k_{\rm s}$ is the split. $\mathrm{s}(t,X_1)$ = 1 means a green light, and $\mathrm{s}(t,X_1)$= 0 means a red light. In this paper, $T_{\rm s}$ and $q_{\rm s}$ is fixed as 80.0 s and 0.4, respectively.

3.2. Evaluation Function and Constraint Condition

The evaluation function and the constraint conditions are described as

$$\min.\ W_{\rm in}=\int_{t_0}^{t_f}P_{\rm in}(\boldsymbol{x}(t),u(t))dt \tag{20}$$

$$s.t.\quad \dot{\boldsymbol{x}}(t)=\boldsymbol{f}(\boldsymbol{x}(t),u(t)), \tag{21}$$

$$\chi(\boldsymbol{x}(t_0))=\boldsymbol{x}(t_0)-\boldsymbol{x}_0=\boldsymbol{0}, \tag{22}$$

$$\psi(\boldsymbol{x}(t_f))=\boldsymbol{x}(t_f)-\boldsymbol{x}_f=\boldsymbol{0}, \tag{23}$$

$$X(t)\leqq X_1\quad(\,t\leqq(1-q_s)T_s\,), \tag{24}$$

$$\boldsymbol{x}(t)=\left[\ V(t),X(t)\ \right]^{\rm T},u(t)=F_{\rm all}(t), \tag{25}$$

where $W_{\rm in}$ is the total energy consumption, $P_{\rm in}$ is the inverter input power, V is the vehicle velocity, X is the distance traveled, $F_{\rm all}$ is the total driving force. $\boldsymbol{x_0}$ and $\boldsymbol{x_f}$ are the initial and final state, respectively. In this paper, steepest descent method is used to calculate vehicle velocity trajectory to solve the nonlinear optimization problem [(?)].

3.3. Comparison Conditions

To verify the performance of the proposed method, it is compared with two velocity profiles which are regraded as the conventional methods. One is a simple optimized trajectory with the traffic signal information. The other calculates the nonlinear optimization without the traffic signal information.

3.3.1. Conventional Profile 1: Constant Acceleration and Deceleration with Signal Information

The conventional profile 1 is composed of constant acceleration, constant speed and constant deceleration as shown in Eq. (**??**).

$$V(t,V_c)=\begin{cases}V_0-a_1t & (0\leq t\leq t_s),\\ V_{\rm s}+a_2(t-t_s) & (t_s\leq t\leq t_1),\\ V_{\rm c} & (t_1\leq t\leq t_2),\\ V_{\rm c}-a_2(t-t_2) & (t_2\leq t\leq t_f).\end{cases} \tag{26}$$

It minimizes energy consumption by autonomous driving using the traffic signal information, witch means that X_1, T_s and q_s are assumed to be known. Then the parameter of Eq. (**??**)–(**??**) are defined as

$$t_s=(1-q_s)T_s, \tag{27}$$

$$a_1=\frac{V_0t_s-X_1}{t_s^2/2}, \tag{28}$$

$$V_s=-a_1t_s+V_0, \tag{29}$$

$$a_2=\frac{1}{2}\frac{-2{V_c}^2-{V_s}^2+2V_sV_c}{X_f-X_1-V_c(t_f-t_s)}, \tag{30}$$

$$t_1=-\frac{V_s-V_c}{a_2}+t_s, \tag{31}$$

$$t_2=t_f-\frac{V_c}{a_2}. \tag{32}$$

3.3.2. Conventional Profile 2: Optimized Velocity Profile without Signal Information

The conventional profile 2 minimizes energy consumption by autonomous driving, considering the traffic signal phase. We assume that vehicle gets the signal phase by not ITS communication

Copyright © 2016 Society of Automotive Engineers of Japan, Inc. All rights reserved

Table 3: Total Energy Consumption [kWs] (Simulation results).

Conventional 1	Conventional 2	Proposed
53.1	61.6	44.3

but the in-vehicle camera. When the in-vehicle camera captures a red light, the vehicle will use the conventional READ without time constraint strategy [(?)] . The conventional profile 2 is calculated to minimize energy consumption from X_0 to X_1 without time constraint strategy. When the light turns a green light, the velocity trajectory will change to the conventional READ with time constraint strategy [(?)] which is calculated to minimize energy consumption from $X(t_s)$ to X_f up to t_f

3.3.3. Proposed Profile: Optimized Velocity Profile with Signal Information

Proposed profile minimizes energy consumption by autonomous driving, using the traffic signal information. The optimal trajectory of $\boldsymbol{x}(t)$ is obtained at the starting point to minimize total energy consumption Eq. (**??**) with constraint Eq. (**??**)–(**??**).

4. Simulation

Simulation results are shown in Fig. **??**. A red star in Fig. **????** means the point where the traffic signal changes from a red light to a green light.

To analyse the simulation results, mechanical output $P_{\rm out}$ is separated into the power stored as kinetic energy of vehicle mass $P_{\rm M}$, the sum of the power stored as rotational energy of each wheel $P_{\rm J}$, the loss caused by the driving resistance $P_{\rm R}$, and the sum of the loss caused by slip of each wheel $P_{\rm S}$. The integrated values of these values are described as

$$W_{\rm X} = \int_{t_0}^{t_f} P_{\rm X}(\boldsymbol{x}(t), u(t))dt, \tag{33}$$

where the subscript X represents “ out ”, “ M ”, “ J ”, “ R ”, “ S ”, “ c ”, and “ i ” as explained previously.

As shown in Fig. **????**, in the conventional profile 1, the vehicle stops at the traffic signal. Vehicle accelerates to about 30 $\rm km/h$ near the traffic signal and stops at goal point.

In the conventional profile 2, when the in-vehicle camera captures a red light, the vehicle decelerates optimally to stop at the traffic signal. The conventional profile 2 prevents the vehicle from losing kinetic energy by the driving resistance loss. The conventional profile 2 reduces more driving resistance loss than the conventional profile 1 as shown Fig. **????** When the light turns a green light, the vehicle accelerates optimally to about 45 $\rm km/h$ and stops goal point to minimize energy consumption from $X(t_s)$ to X_f. It prevents the vehicle from causing motor loss and driving resistance loss. However total driving force and velocity of the conventional profile 2 are larger than those of the conventional profile 1 and proposed profile. It increases more iron loss, copper loss and driving resistance loss than the conventional profile 1 as shown Fig. **????**–Fig. **????**. Therefore total energy loss of the conventional profile 2 is largest in three velocity profiles as shown Fig. **????**.

On the other hand, in the proposed profile, during the red light, the vehicle reduces speed at an optimal deceleration and travels at a low speed to the point of the traffic signal. The proposed profile reduces more driving resistance loss than the conventional profile 1 and 2 as shown Fig. **????**. When the light turns a green light, kinetic energy of proposed profile is larger than that of the conventional 1 and 2. Then the proposed profile did not need

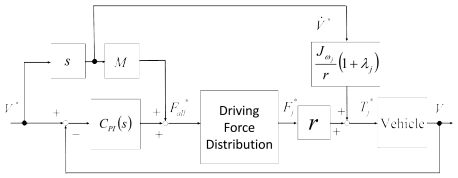

Fig. 6: Vehicle velocity control system.

to accelerate more largely than the conventional profile 1 and 2. Therefore it reduces more copper loss than the conventional profile 1 and 2 as shown Fig. **????**.

Energy consumption of the conventional profile 1, 2 and proposed profile is 53.1 kWs, 61.6 kWs, 44.3 kWs, respectively, as shown Fig. **????** and Tab. **??**. Energy consumption of the proposed profile improves significantly 16.6 % and 28.1 % compared with that of the conventional profile 1 and 2.

Fig. **????** shows total energy loss which is composed of copper loss, iron loss, slip loss and driving resistance loss. Copper loss is proportional to the square of total driving force as shown Eq. (**??**). As shown Fig. **????**, total driving force of the proposed profile is smallest in three profiles from t_s to t_f. Therefore copper loss of proposed profile reduces significantly 56.0 % and 69.7 % compared with that of the conventional profile 1 and 2. Iron loss is proportional to the square of total driving force and velocity as shown Eq. (**??**). As shown Fig. **????** and Fig. **????**, total driving force and velocity of the proposed profile are smallest in three profiles from t_s to t_f. Therefore iron loss of proposed profile reduces significantly 0.452 % and 4.15 % compared with that of the conventional profile 1 and 2. Driving resistance loss is proportional to the square of velocity as shown Eq. (**??**). As shown Fig. **????**, velocity of the proposed profile is smallest in three profiles from t_s to t_f. Therefore driving resistance loss of proposed profile reduced significantly 2.05 % and 10.8 % compared with that of the conventional profile 1 and 2.

5. Experiment

5.1. Control System

Vehicle velocity control system is designed to control the EVs velocity automatically. Fig. **??** shows the system which is composed of a feedforward controller and feedback controller. Front and rear torque reference $T_j{}^*$ is given as

$$T_j{}^* = rF_j{}^* + \frac{J_{\omega_j}\dot{V}^*}{r}(1+\lambda_j). \tag{34}$$

The second term of right hand side compensates inertia torque of the wheels. Vehicle velocity controller $C_{PI}(s)$ is a PI controller, and it is designed by the pole placement method. The closed–loop pole is allocated to -5 $\rm rad/s$

5.2. Experiment Environment

Experiments were conducted on both the Real Car Simulation bench test (RC–S) and driving test road shown in Fig. **??** under the same condition as simulations. RC-S developed by ONO Sokki Co., Ltd. can reproduce various travel situation without being influenced by change of wind and road surface condition. Vehicle velocity V and inverter input power $P_{\rm in}$ are calculated as

$$V = \frac{r}{4}\sum_{j=f,r}\sum_{i=l,r}\omega_{ij}, \tag{35}$$

$$P_{\rm in} = V_{\rm dc}\sum_{j=f,r} I_{{\rm dc}j}, \tag{36}$$

Copyright © 2016 Society of Automotive Engineers of Japan, Inc. All rights reserved

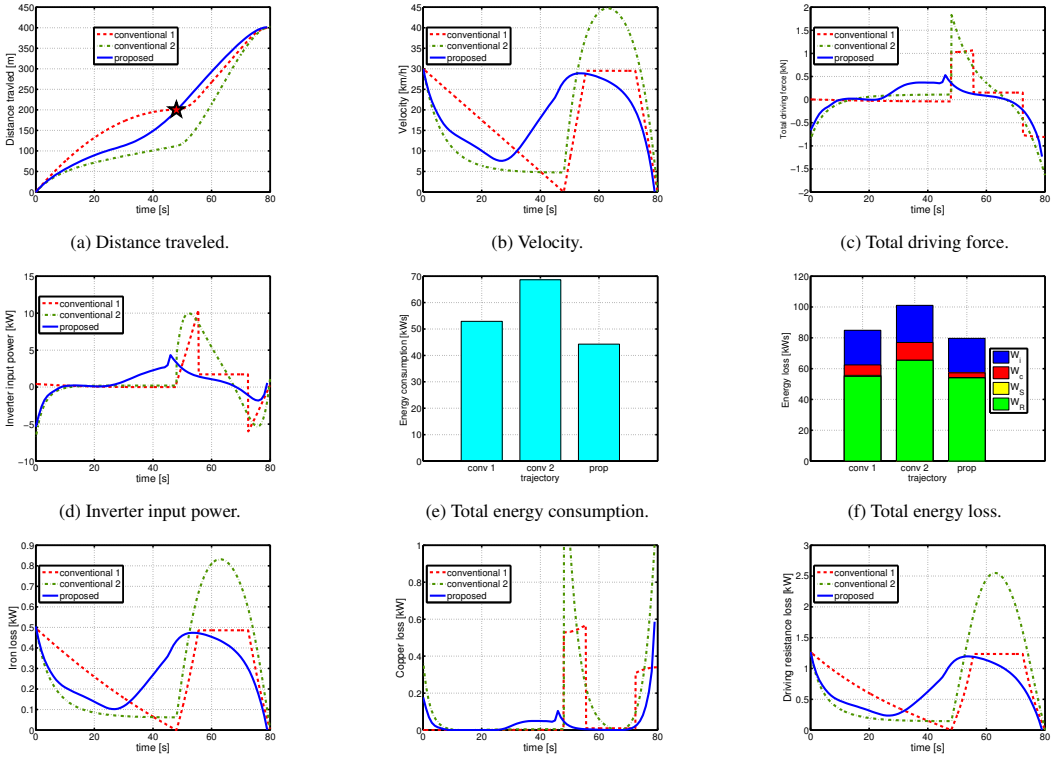

(a) Distance traveled. (b) Velocity. (c) Total driving force.

(d) Inverter input power. (e) Total energy consumption. (f) Total energy loss.

(g) Iron loss. (h) Coppoer loss. (i) Driving resistance loss.

Fig. 5: Simulation Results.

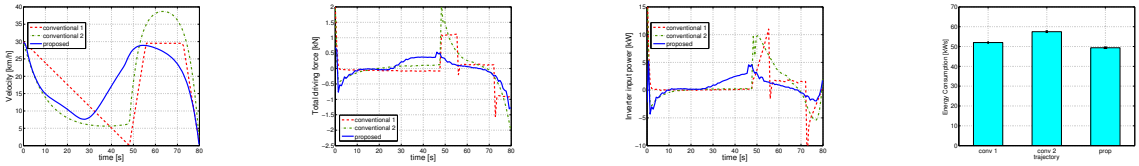

(a) Velocity. (b) Total driving force. (c) Inverter input power. (d) Consumption energy.

Fig. 8: Experiment results of RC-S.

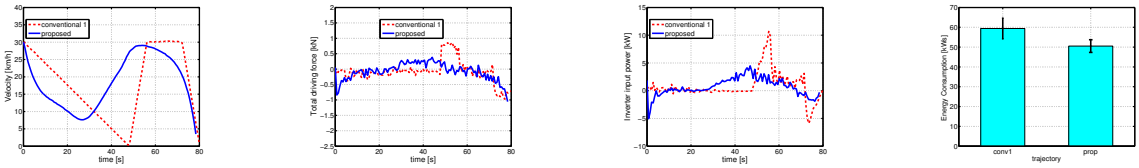

(a) Velocity. (b) Total driving force. (c) Inverter input power. (d) Consumption energy.

Fig. 9: Experiment results of driving test.

(a) Real Car Simulation bench test (RC–S). (b) Driving test road.

Fig. 7: Experiment environment.

where the subscript i represents l or r (l stands for left and r represents right wheel). V_{dc} is measured the inverter input voltage and $I_{\mathrm{dc}j}$ is the measured inverter input current. P_{in} includes inverter loss.

Table 4: Total energy consumption [kWs] (Average±Standard deviation) .

	Conventional 1	Conventional 2	Proposed
RC–S	52.0±0.423	57.5±0.415	49.4±0.343
Driving test	59.4±5.19	N/A	50.5±3.18

5.3. Experiment Results of RC–S

Experiments were conducted on the RC–S under the same condition with simulations. Fig. **??** shows experimental results. Fig. **????** and Tab. **??** shows total energy consumption which is the

Copyright © 2016 Society of Automotive Engineers of Japan, Inc. All rights reserved

average values and standard deviations of the experiments repeated four times.

Total energy consumption of the conventional profile 1, the conventional profile 2 and proposed profile is 52.0 kWs, 57.5 kWs, 49.4 kWs respectively. Average total energy consumption of the proposed profile improved significantly 5.02 % and 14 .1% compared with that of the conventional profile 1 and 2. Average total energy consumption differs from that of simulation result because neglecting inverter loss and chopper loss affect modelling error of power flow model. The experimental results are consistent with simulation results.

5.4. Experiment Results of Driving Teset

Experiments were conducted on driving test road under the same condition as simulations. The test road restricts a speed to a prescribed value 30 km/h or less. We were not able to have experiments of the conventional profile 2. Fig. **??** shows experimental results. The absolute value of total driving force differs from simulation result because of modelling error of driving resistance, as shown in Fig. **????**. Fig. **????** and Tab. **??** shows total energy consumption which is the average values and standard deviations of the experiments repeated four times.

Total energy consumption of the conventional profile 1 and the proposed profile are 59.4 kWs and 50.5 kWs, respectively. Average total energy consumption of the proposed profile improved significantly 14.9 %compared with that of conventional profile 1 and 2. Vehicle which travelled in test drive was affected by road surface disturbance while vehicle was not affected by road surface disturbance in RC–S bench test. RC–S represents the driving resistance during travelling by Eq. (**??**). Therefore average total energy consumption of the driving test was different from that of RC–S. However the experimental results of driving test are consistent with simulation results and experiment results of RC–S. Experiments verified that the proposed profile is superior to conventional profile 1 and 2 not only simulation but also the driving test.

6. Conclusion

In this paper, we propose READ by considering the traffic signal from one traffic light. Proposed READ system reduces more energy consumption than that of the conventional profile in simulations and experiments. The future works include considering the space between a car and the one in front.

Acknowledgement

This research was partly supported by Industrial Technology Research Grant Program from New Energy and Industrial Technology Development Organization (NEDO) of Japan (number 05A48701d), the Ministry of Education, Culture, Sports, Science and Technology grant (number 22246057 and 26249061), and the Core Research for Evolutional Science and Technology, Japan Science and Technology Agency (JST-CREST). This result is a part of work in the project team of JST-CREST named "Integrated Design of Local EMSs and their Aggregation Scenario Considering Energy Consumption Behaviors and Cooperative Use of Decentralized In-Vehicle Batteries.

References

(1) Y. Hori:"Future Vehicle Driven by Electricity and Control–Research on Four–Wheel–Motored" UOT Electric March II"," IEEE Trans. on Industrial Electronics, Vol. 51, No. 5, pp.954–962 (2004).

(2) H. Hijikata, K. Akatsu, Y. Miyama, H Arita, and A. Daikoku:"Suppression Control Method for Iron Loss of MATRIX Motor under Flux Weakening Utilizing Individual Winding Current Control," The 7th International Power Electronics Conference, IPEC-Hiroshima 2014 - ECCE Asia-, pp. 2673–2678 (2014).

(3) R.Nakajima, R.Koyama, D.Matsuoka, Y.Kano, and M.Abe:"The Effects of tire force distribution control on reducing tire slip energy dissipation," 2013 JSAE Annual Congress (Spring), No. 30, pp. 21–24 (2013). (inJapanese)

(4) T.Kobayashi, E.Katsuyama, H.Sugiura, E.Ono, and M.Yamamoto:"Study on Driving Force Distribution and Power Consumption in Cornering : Formulation for Steady State Cornering and Validation Using EV," JSAE Transaction, Vol. 45, No. 2, pp. 309–314 (2014). (inJapanese)

(5) O.Nishihara, T.Kumazawa:"ElectricPower Conservationby Driving/Braking Force Distribution in Electric Vehicle," Dynamics and Design Conference, pp. 330–1–300–6 (2010).(inJapanese)

(6) H. Fujimoto and S. Harada:"Model-Based Range Extension Control System for Electric Vehicles With Front and Rear Driving–Braking Force Distributions," IEEE Trans. on Industrial Electronics, Vol. 62, No. 5, pp. 3245–3254 (2015).

(7) H. Kimura, H. Otake, H. Oguri and M. Kanematsu:"Field Evaluation Test Results of Green Wave Advisory System," Society of Automotive Engineers of Japan, Inc., No. 87–12, pp. 15–18 (2012). (in Japanese)

(8) M. A. S. Kamal, M. Mukai, J. Murata, and T. Kawabe:"Model Predictive Control of Vehicles on Urban Roads for Improved Fuel Economy," IEEE Trans. on Control Systems Technology, Vol. 21, No. 3, pp. 831–841 (2013).

(9) X. Wu, X. He, G. Yu, A. Harmandayan, and Y. Wang:"Energy-Optimal Speed Control for Electric Vehicles on Signalized Arterials," IEEE Trans. on Intelligent Transportation Systems, pp.1–11 (2015).

(10) S. Harada and H. Fujimoto: "Range Extension Control System Based on Optimization of Acceleration-Deceleration profile and Front and Rear Driving-Braking Force Distribution," Multi-symposium on Control Systems, 6F1–4 (2014) (in Japanese).

(11) H. Yoshida and H. Fujimoto:"Range Extension Autonomous Driving for Electric Vehicles Based on an Optimal Vehicle Velocity profile Considering Road Gradient Information," The 1st IEEJ International Workshop on Sensing Actuation and Motion Control (SAMCON), pp. 1 –6 (2015).

(12) Y. Ikezawa, H. Fujimoto, and Y. Hori:"Range Extension Autonomous Driving for Electric Vehicles Based on Optimal Vehicle Velocity profile Generation and Front–Rear Driving–Braking Force Distribution with Time Constraint," The 1st IEEJ International Workshop on Sensing Actuation and Motion Control (SAMCON), pp. 1–6 (2015).

(13) H. B. Pacejka and E. Bakker:"The Magic Formula Tyre Model," Vehicle System Dynamics, International Journal of Vehicle Mechanics and Mobility, Vol. 21, No. 1, pp. 1–18 (1992).

(14) T. Ohtsuka: "Introduction to Nonlinear Optimal Control," CORONA PUBISHING CO., LTD. (2011)(in Japanese)

(15) D. Kawano, Y. Goto, K. Echigo, and K. Sato:"Analysis of Behavior of Fuel Consumption and Exhaust Emissions under On–road Driving Conditions Using Real Car Simulation Bench (RC–S)," 2009 JSAE Annual Congress (Spring), Vol. 19, pp. 9–12 (2009) (in Japanese).

Copyright © 2016 Society of Automotive Engineers of Japan, Inc. All rights reserved